JOURNAL OF MATERIALS SCIENCE **39** (2004) 1105–1107

Properties of CoSb as the anode material for rechargeable lithium ion batteries

J. XIE, G. S. CAO, X. B. ZHAO*, M. J. ZHAO, Y. D. ZHONG, L. Z. DENG, Y. H. GUAN, Z. T. WU
Department of Materials Science and Engineering, Zhejiang University, Hangzhou 310027, People's Republic of China
E-mail: Zhaoxb@zju.edu.cn

Lithium ion secondary batteries are now the prevailing rechargeable batteries due to their high working-voltage and high-energy density. Commercial lithium ion batteries use $LiCoO_2$ and graphite as cathode and anode materials, respectively. Lithium-alloys [1–3] have received great interest because of their higher packing density than that of carbon-based materials, since they obey a lithiation/delithiation mechanism rather than an intercalation/disintercalation mechanism. However, the lithium alloys with high energy density have not entered the commercial markets yet. The major shortcoming of lithium alloys is that they suffer from insufficient long-term cycling stability due to the large volume changes from the active species (Sb, Sn and Si etc.) alloying/dealloying with Li, which often causes anode cracking and pulverization.

It has been reported that this drawback can be overcome partly by using intermetallic compounds [4–8], instead of pure metals. The intermetallic compounds exhibit slightly smaller Li-storage capacity than the pure metals, but often show an improved cycling stability. Generally, the intermetallic compound consists of an active species and an inactive species. It is believed that the active species can electrochemically react with Li when polarized to the sufficiently low potential and provides the anode capacity, while the inactive species offers an inert matrix to support the active species and alleviates the volume effect associated with the active species during the charge and discharge cycling.

Based on the above concept, some Sb-based intermetallic compounds [9–11] have been suggested as promising anode materials for secondary lithium ion batteries in our group. In our present work, the CoSb compound was prepared by levitation melting and the electrochemical performance of CoSb as an alternative anode material for secondary lithium ion batteries was investigated.

The stoichiometric mixture of pure Sb and pure Co was sealed in the copper crucible for evacuation under 0.1 Pa. The metals were levitated in the crucible under Ar atmosphere and alloyed by the diffusion mixing effect of the intensive stirring of the electromagnetic force produced by high frequency eddy current. The as-cast alloy ingot was annealed at 500 °C for 7 days and was ground into 50 μm fine powder. The powder was further milled with a planetary ball-milling machine for 24 h at a rotation rate of 230 rpm. The morphology of the ball-milled CoSb powder was observed by a Philips SEM model 501B. The milled CoSb powder was characterized by X-ray diffraction (XRD) using a Philips PW 1770 powder diffractometer equipped with Cu K_α radiation.

A slurry consisting of 5 wt% acetylene black as the conducting additive, 10 wt% PTFE (polytetrafluoroethylene) as the binder and 85 wt% ball-milled CoSb powders was coated onto foam Ni matrix as working electrode. The electrodes were dried under vacuum at 120 °C overnight before assembling into the cells in an Ar-filled glove box. The model cell was constructed by using metallic lithium as the counter electrode, 1 M $LiPF_6$ in EC (ethylene carbonate)/DMC (dimethyl carbonate) (1:1 v/v) as the electrolyte and PP (polypropylene) microporous film Cellgard 2300 as the separator. The cells were charged and discharged between 0.05–1.5 V versus Li/Li^+ at a constant current density 40 mA g^{-1}.

Electrochemical impedance spectroscopy (EIS) measurements were performed using a Solartron FRA 1250 frequency response analyzer combined with a Solartron SI 1287 electrochemical interface. Impedance spectra were recorded potentiostatically by applying an ac voltage of 5 mV amplitude over the frequency range from 120 kHz to 5 mHz after the cells have left for 24 h to achieve equilibrium. *Ex situ* XRD was executed on the electrodes at different charge and discharge states to study the electrochemical reaction mechanism of CoSb with Li. The cells were dismantled in the glove box and the electrodes were covered with a PE (polyethylene) film to avoid exposing in air.

Fig. 1 shows the SEM image of ball-milled CoSb powder. The XRD pattern of CoSb alloy powders after being annealed and ground is presented in Fig. 2. Note that after annealing, a dominant phase of CoSb is obtained. However, the Sb diffraction peaks are also observed in the pattern.

The electrochemical performance of CoSb alloy was evaluated using $Li/LiPF_6$ (EC + DMC)/CoSb model cells. Fig. 3 shows the voltage profiles of CoSb alloy for the initial two charge and discharge cycles. As seen from the figure, CoSb shows a large first discharge (Li-alloying) capacity. The rapid drop of potential, mainly between 1.5 and 0.75 V, is supposed

* Author to whom all correspondence should be addressed.

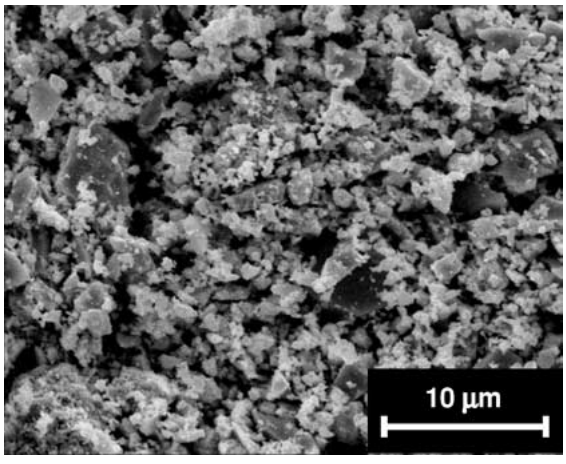

Figure 1 SEM image of ball-milled CoSb powder.

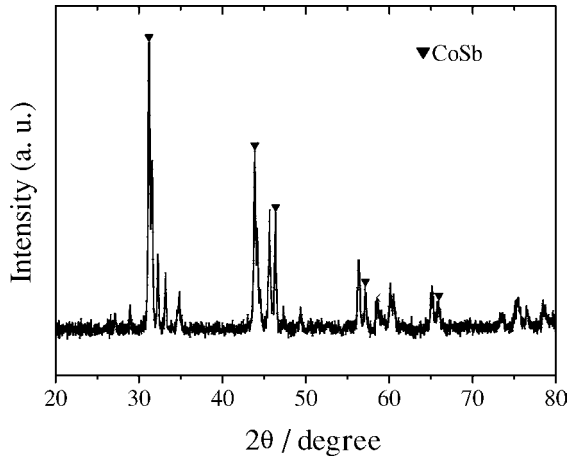

Figure 2 XRD pattern of CoSb annealed and ground to a powder.

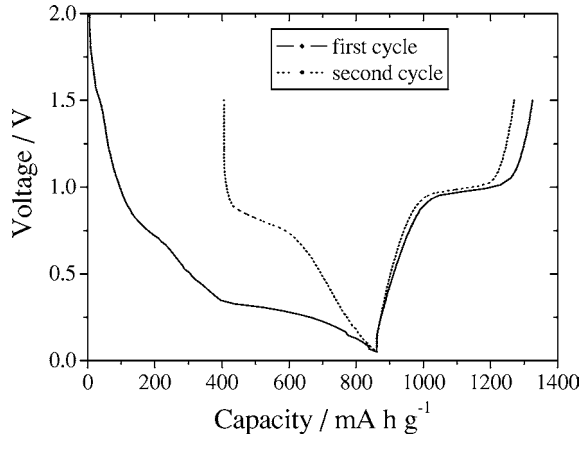

Figure 3 Voltage profiles of CoSb electrodes for the first two cycles.

to be caused by the decomposition of electrolyte and formation of solid electrolyte interface (SEI) on the surface of alloy or metal particles. The ball-milled alloy particles have large specific surface area, which facilitates the decomposition reactions of electrolyte on their surface. The decomposition products, which consist mainly of Li_2CO_3 and $(CH_2OCO_2Li)_2$ when EC-based electrolyte solution was used as reported by Aurbach *et al.* [12], formed the SEI film. This can explain the large irreversible capacity during the first discharge process. Two potential plateaus located at about 0.75 and

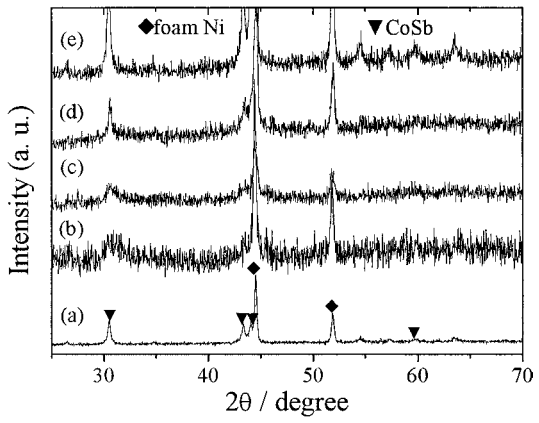

Figure 4 Ex situ XRD patterns of CoSb electrodes at the different states: (a) fresh electrode, (b) discharge to 0.8 V, (c) discharge to 0.05 V, (d) charge to 1.0 V, and (e) charge to 1.5 V.

0.25 V, respectively, are observed for the CoSb alloy. The first plateau can be ascribed to lithium-alloying reactions of Sb impurity in the CoSb sample, while the second one is due to the breakdown of CoSb structure and the formation of Li_3Sb. It is found that the subsequent charge and discharge cycles are reproducible, namely, the charge and discharge plateaus are fixed at 1.0 and 0.8 V, respectively. This means after the first discharge, reversible reactions occur.

To study the electrochemical Li-storage mechanism, we carried out *ex situ* XRD measurements on the CoSb electrodes at the different charge and discharge potentials. The evolutions of the XRD patterns are collected in Fig. 4. The CoSb is subjected to progressive amorphization upon charge and discharge process. However, the expected Li_3Sb phase is not well resolved even on the deep discharge stage. We believe that it may exist in the amorphous state. By charging (dealloying) to 1.5 V versus Li/Li^+, the CoSb reflections emerge again. This means the reaction of CoSb with Li is reversible after the first discharge, namely, Li is extracted from Li_3Sb and the CoSb structure is reconstructed.

The reversible (Li-dealloying) capacity as a function of cycle number for CoSb is given in Fig. 5. As expected, the cycleability of CoSb alloy has been significantly improved compared with that of pure Sb [13], even though it exhibits a relative smaller reversible

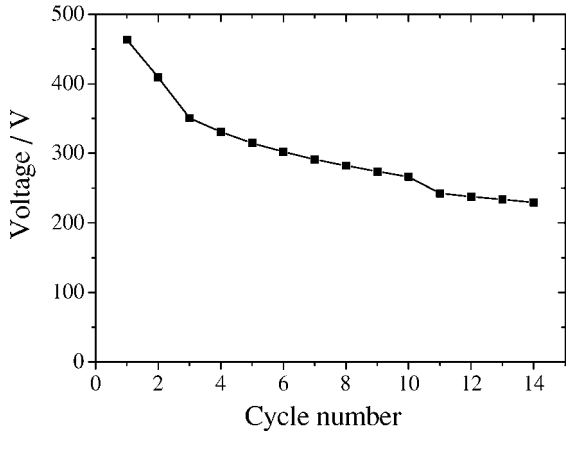

Figure 5 Cycleability of CoSb electrodes at the current density of 40 m Ag^{-1}.

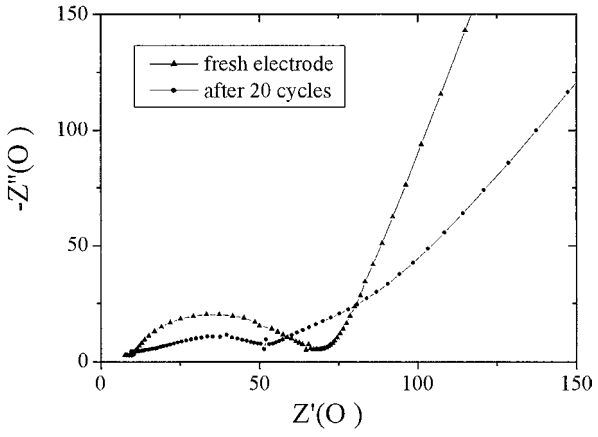

Figure 6 EIS of CoSb electrodes in 1 M $LiPF_6$ in 1:1 EC/DMC.

capacity in the initial several cycles. The enhancement of cycling stability of CoSb can be attributed to the "separator" effect of Co matrix. We believe that Li_3Sb can be finely distributed in the Co matrix during the discharge processes. In addition, the boundaries between Co and Li_3Sb make the diffusion of Li-ions in the electrode easier. Nevertheless, the volume expansion/contraction accompanying lithium alloying/dealloying is serious and generates mechanical stress in the electrode, which limits the cycle life of the batteries. As a result, the alloy materials still cannot compete with the commercial carbon-based materials, since they obey an alloying/dealloying mechanism rather than an intercalation/deintercalation mechanism.

EIS was used to investigate impedance changes of CoSb before and after cycling. As indicated in Fig. 6, before cycling, the impedance spectra show a well-defined semicircle in the high and middle frequency range and a straight line at the low frequency corresponding to the Warburg impedance. After cycling, the well-defined semicircle turns into a depressed semicircle, which can be characteristic of two partially overlapped semicircles. According to Kang *et al.* [14], the first semicircle at high frequency is due to the formation of SEI layer on the surface of the alloy particles, while the second one corresponds to the charge transfer behavior. As a result, the EIS results further confirm the existence of SEI film on the CoSb particles.

Acknowledgments

The work is supported by National Natural Science Foundation of China (No. 50201014) and PFDP of the Education Ministry of China (No. 20010335045).

References

1. J. WANG, I. D. RAISTRICK and R. A. HUGGINS, *J. Electrochem. Soc.* **133** (1986) 457.
2. M. WINTER and J. O. BESENHARD, *Electrochim. Acta* **45** (1999) 31.
3. C. J. WEN, B. A. BOUKAMP, R. A. HUGGINS and W. WEPPNER, *J. Electrochem. Soc.* **126** (1979) 2258.
4. L. MONCONDUIT, J. C. JUMAS, R. ALCÁNTARA, J. L. TIRADO and C. P. VICENTE, *J. Power Sources* **107** (2002) 74.
5. H. KIM, Y.-J. KIM, D. G. KIM, H.-J. SOHN and T. KANG, *Sol. State Ion.* **144** (2001) 41.
6. I. ROM, M. WACHTLER, I. PAPST, M. SCHMIED, J. O. BESENHARD, F. HOFER and M. WINTER, *ibid.* **143** (2001) 329.
7. J. WOLFENSTINE, S. CAMPOS, D. FOSTER, J. READ and W. K. BEHL, *J. Power Sources* **109** (2002) 230.
8. L. FANG and B. V. R. CHOWDARI, *ibid.* **97/98** (2001) 181.
9. L. J. ZHANG, X. B. ZHAO, X. B. JIANG, C. P. LV and G. S. CAO, *ibid.* **94** (2001) 92.
10. X. B. ZHAO, G. S. CAO, C. P. LV, L. J. ZHANG, S. H. HU, T. J. ZHU and B. C. ZHOU, *J. Alloys Comp.* **315** (2001) 265.
11. G. S. CAO, X. B. ZHAO, T. LI and C. P. LU, *J. Power Sources* **94** (2001) 102.
12. D. AURBACH, M. D. LEVI, E. LEVI and A. SCHECHTER, *J. Phys. Chem.* B **101** (1997) 2195.
13. K. C. HEWITT, L. Y. BEAULIEU and J. R. DAHN, *J. Electrochem. Soc.* **185**(5) (2001) A402.
14. Y.-M. KANG, S.-C. PARK, Y.-S. KANG, P. S. LEE and J.-Y. LEE, *Sol. State Ion.* **156** (2003) 263.

Received 11 June
and accepted 7 August 2003